The effect of arch geometry on the structural behavior of masonry bridges

Ahmet C. Altunışık[*1], Burcu Kanbur[1] and Ali F. Genç[2]

[1]*Department of Civil Engineering, Karadeniz Technical University, Trabzon, Turkey*
[2]*Department of Civil Engineering, Karadeniz Technical University, Of Technology Faculty, Trabzon, Turkey*

Abstract. Arch bridges consist of some important components for structural behavior such as arches, sidewalls, filling materials and foundations. But, arches are the most important part for this type of bridges. For this reason, investigation of arch is come into prominence. In this paper, it is aimed to investigate the arch thickness effect on the structural behavior of masonry arch bridges. For this purpose, Göderni historical arch bridge which was located in Kulp town, Diyarbakır, Turkey and the bridge restoration process has still continued is selected as an application. The construction year of the bridge is not fully known, but the date is estimated to be the second half of the 19th century. The bridge has two arches with the 0.52 cm and 0.69 cm arch thickness, respectively. Finite element model of the bridge is constructed with ANSYS software to reflect the current situation using relievo drawings. Then the arch thickness is changed by increasing and decreasing respectively and finite element models are reconstructed. The structural responses of the bridge are obtained for all arch thickness under dead load and live load. Maximum displacements, maximum-minimum principal stresses and maximum-minimum elastic strains are given with detail using contours diagrams and compared with each other to determine the arch thickness effect. At the end of the study, it is seen that the maximum displacements, tensile stresses and strains have a decreasing trend, but compressive stress and strain have an increasing trend by the increasing of arch thickness.

Keywords: arch bridge; arch thickness; finite element model; structural response

1. Introduction

Historical structures are the identity of the community. They aren't only structures which are contain stone, timber, mortar, etc., they are also contain the social culture and this is the biggest difference between new structures and historical structures. They have big value in human life. Almost every person is curious past and they want to learn some information of their ancestors. So the easiest way to learn about past is to examine the historical data and structures. In the last century, people have given more attention to preserve the historical structures. A lot of studies have carried out for estimating behavior of these structures and could be made reliable restoration to preserve them to future.

Arch bridges hold an important place in historical structures. Historical masonry bridges are one of the primary engineering structures constructed by people. There are a lot of historical

---

∗Corresponding author, Ph.D., E-mail: ahmetcan8284@hotmail.com

bridges constructed in various sizes, styles and spans all over the world. Some of them are nearly as old as a couple of thousands years (Bayraktar *et al.* 2009). They aren't complex structures. A stone arch bridge consists of stone blocks and mortar joints. Blocks have high strength in compression and low strength in tension while mortar has generally low strength.

Historical masonry arch bridges are vital components of transportation systems in many countries worldwide, ensuring the ready access of goods and services to millions of people (Sevim *et al.* 2010). They were built for different purposes such as social and economical as well as strategic aims (Bayraktar *et al.* 2009). Many of those bridges, which were originally built for the passage of carts, are being used for road and rail vehicles. They demonstrate a surprisingly high load bearing capacity and good durability. For these reasons, several ancient arch bridges are still in use today, even if the most part is relatively recent (19th century). Still, with time, masonry bridges have deteriorated and the safety requirements changed. The axle loads, number of axles and the vehicle speed the bridges are subjected to, have changed significantly in the past century. For this reason, countries have made a lot of reinforcement and restoration application for reliable use of bridges under current situations.

Arch is the most important part of masonry bridges. Arch form is most possibly one of the oldest architectural forms used for bridge type structures, especially for masonry bridges (Bayraktar *et al.* 2010). A lot of arch forms have been existed in bridges life. Arches and vaults is used to pass long spans during thousand years. The first arches were found in underground tombs in Mesopotamia, built around 3000 BC (Oliveira *et al.* 2010). Investigation of arch type takes a big place for understood the bridge behavior.

Many studies exist in the literature about the structural behavior of historical bridges including analyses type, different load cases and reinforcement restoration techniques using analytical and experimental methods (Ural *et al.* 2008, Cancelliere *et al.* 2010, Tao *et al.* 2011, Pelà *et al.* 2013, Caporale *et al.* 2014). Toker and Unay (2004) made a prototype model of a bridge then studied about mathematical modeling techniques on it under different loading conditions. Bayraktar *et al.* (2007) investigated the effect of finite element model updating on earthquake behavior of historical bridges. Brencich and Sabia (2008) studied on the Tanaro Bridge which has 18 spans. The bridge was investigated accordance both the service conditions and different stages of demolition. The dynamic characteristics of the bridge were gained with dynamic tests. Altunışık *et al.* (2011) studied on the finite element updating by means of vibration-based operational modal analysis. Mikron masonry arch bridge is used for study. Oliveira *et al.* (2010) made a geometrical survey on 59 segmental masonry arch bridges from Portugal and Spain. Historical empirical rules for shape of arch, thickness of arch and width of piers are briefly presented and further compared against the bridges' geometrical data. Eight reference bridges are defined as representative of the sample. Then assessment of the load-carrying capacity of the reference bridges and a discussion of results are made. Sayın *et al.* (2011) constituted a 3D finite element model of historical Uzunok Bridge and examine the linear and nonlinear analysis. Arteaga and Morer (2012) investigated the effect of geometry on the structural capacity of masonry arch bridges with different geometric features. Study aims to estimate the percentage of error that can occur in the structural assessment of masonry bridges by reading from different shapes as well as to estimate geometrical error. Cakir and Uysal (2014) displayed the composite polymer material effect on the damping ratios and frequencies.

Geometry has an important place in masonry structures and especially masonry arch bridges. With the increasing of loads, this issue becomes more important for restorations and reinforcement. It can be easily seen that some studies are performed about the investigation of bridge geometry

with accordance to empiric formulas. Investigations and comparisons are made to be relationship between different parameters and considered the empiric formulas. In this study, it is aimed to investigate the arch thickness effect on the structural behavior of masonry arch bridges. Arch thickness is changed by increasing and decreasing respectively. Nine different arch thicknesses were evaluated under dead loads and live loads for comparison. Maximum displacements, maximum-minimum principal stresses and maximum-minimum elastic strains are given with detail using contours diagrams and compared with each other to determine the arch thickness effect.

2. Numerical application

Göderni masonry arch bridge is located on the Sarum brook in the 30km north of Kulp town of Diyarbakır, Turkey. Construction year of the bridge is not fully known, but the bridge is dated back to 19th century. The bridge has two segmental arches with yellowish colored cut stone. Göderni Bridge, located into bowless bridge group and having the same characteristics in terms of arch form, is built in larger measure than others.

The main structural elements of the bridge (stone arch, side walls and timber block) have damaged at specific regions and have not been repaired yet. For this reason, the restoration is planning for the bridge by general directorate of highways. After restoration projects and studies, it is planned to opening of the bridge for pedestrian crossings and traffic. Fig. 1 shows the some views of Göderni Bridge.

The bridge has two arches. Total length and width of the bridge are 62.00 m and 6.05 m, respectively. Maximum span and heights of the first and second arches are 12.00 m-11.85 m and 3.04 m-3.26 m, respectively. The distance between water level and inner surface of arches are 11.31m and 11.73 m for first and second arches. First arch radius and thickness are 7.54 m and 0.52 m, respectively. But, the second arch has two center points and radius as 9.35 m and 9.37 m, the thickness of the arch is 0.69 m. The thickness of the side walls is 0.5 m. The timber block between two side walls has 5.05 m width. The pavement consists of sand, gravel and pressed soil.

Fig. 1 Some views of Göderni historical masonry arch bridge

3. Determination of the material properties

Göderni Bridge is a masonry stone arch bridge. The masonry bridges have different material like mostly stone, mortar, steel and wood which can be used for several purposes. Every part of arch requires carefully labor and specific materials for built. On this bridge, the arches are built with cut stone and side walls are built mostly cut stones and different type of stones. The timber blocks between side walls consists of variable sizes of limestone, sand and gravel. Cement-based mortar is used as a binding material.

Stone and mortar samples are taken from the bridge for determine the mechanical properties of materials used in the bridge and are tested in the laboratory. As a result of the tests, the mechanical properties were obtained and they were used to compare and control with results of finite element analysis. The compressive strength and weight per unit volume were measured as 30-50MPa and 2000-2400 kg/m^3 for stones, respectively. Also, the compressive strength of the mortar was defined as 4-9MPa.

4. Structural analysis of the bridge under diffreent arch thickness

Finite element analyses are carried out to determine and compare the structural behavior of the bridge under different arch thickness using relievo drawings. General information, structural dimensions, material properties and some additional information of the bridge are acquired from the Abdulkadir Aslan Engineering Company. Finite element models of the bridge were constituted using ANSYS software (ANSYS, 2014).

Nine different structural analyses were planned to determine the arch thickness affect more accurately. For better understanding, the first analyses are performed using relievo drawings. It is seen that first and second arches have 0.52 m and 0.69 m thickness, respectively. The arch thicknesses are increased and decreased as 10cm for each analysis. The detail information can be seen in Table 1. Maximum displacements, maximum-minimum principal stresses and maximum-minimum elastic strains are given with detail for first analyses using relievo drawings. The changing of these results under different arch thickness are displayed using tables and figures.

The selected analyses case to determine the structural behavior is listed below:

- *Dead load for nine different arch thicknesses*
- *Dead load and live loads for nine different arch thicknesses*

In the finite element models of the bridge, SOLID186 solid elements were used. The element had 20 node and three degrees of freedom per node: translations in the nodal x, y, and z directions. In addition it had the capability of plasticity, elasticity, creep, stress stiffening, large deflection, and large strains (ANSYS, 2014). SOLID186 element has tetrahedral, pyramid or prism options for meshing the structure easily and you can see this options finite element mesh model of bridge. A schematic picture of the SOLID186 element is displayed in Fig. 2.

3D finite element model of the bridge (Case 4) is shown in Fig. 3. This model includes 146678 nodes and 87782 mesh elements. These values changed a bit, when the thicknesses of arches were changed. All analyses are made to be linear elastic. All boundary conditions underside of the abutments and edge surfaces of scope volumes are considered to be fixed. Cracked and damaged elements are considered in the finite element models of the bridge.

Table 1 Material properties used in the analytical analysis

Analyses Cases	Arch Thickness	
	First Arch	*Second Arch*
1	0.22 m	0.39 m
2	0.32 m	0.49 m
3	0.42 m	0.59 m
4 (considering relievo drawings)	0.52 m	0.69 m
5	0.62 m	0.79 m
6	0.72 m	0.89 m
7	0.82 m	0.99 m
8	0.92 m	1.09 m
9	1.02 m	1.19 m

Fig. 2 Structural solid geometry of SOLID186 element

In the analysis of masonry structures, the most important issue is determination of the material properties to obtain the current behavior as far as possible. There are some experimental studies and accepted standards in literature about this subject. But, it is difficult to apply these suggestions and assumptions for all structure. Due to these difficulties, the material properties of such kind of structures taken from similar studies in the literature (Frunzio *et al.* 2001, Toker and Unay 2004, Bayraktar *et al.* 2007, Brencich and Sabia 2008, Pelà *et al*. 2013).

During the field investigations on the bridge, some cracks and damages which are effect the structural behavior are observed (Fig. 4).
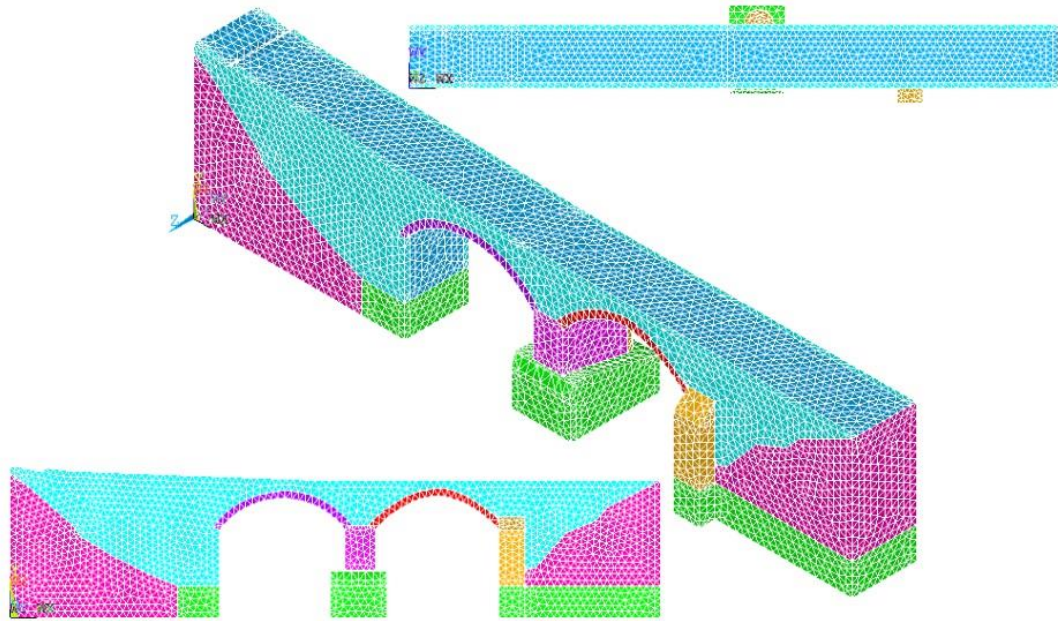
Fig. 3 Finite element model of Göderni masonry arch bridge

- *Damages of arches*
- *Damages of side walls*
- *Damages of pavements/deck*
- *Ruptures of stone pieces*
- *Environmental problems and deteriorations at expansion joints*
- *Existence of vegetation and biological colonization*
- *Scour at abutments*
- *Filling of side slopes*

The material properties considered in the analysis of the bridge are given in Table 2. It can be seen that there are two values for modulus of elasticity. The modulus of elasticity is reduced according to the observed cracks and damages given in above within the acceptable limits considering related articles, thesis and laboratory studies.

Fig. 4 Some views from the field investigations on the bridge

Table 2 Material properties used in the analytical analysis

Structural Elements	Material Properties			
	Modulus of Elasticity (N/m²)		*Poisson Ratio (-)*	Density *(kg/m³)*
	Un-damaged	Damaged		
First Arch	5.00E9	3.25E9	0.20	2000
Second Arch	5.00E9	3.25E9	0.20	2000
Side Walls	3.00E9	1.95E9	0.20	2000
Timber Blocks	6.0E08	3.9E08	0.20	1800
Abutments	5.00E9	3.25E9	0.20	2000
Cutwaters	5.00E9	3.25E9	0.20	2000
Slopes	7.00E9	4.55E9	0.20	2500
Foundations	7.00E9	4.55E9	0.20	2500

Ahmet C. Altunışık, Burcu Kanbur and Ali F. Genç

4.1 Structural response under dead load

The maximum vertical displacements contour diagrams of the bridge for current situation (Case 4) under dead load is shown in Fig. 5. It can be seen from the Fig. 5 that the displacements have an increasing trend from side abutments and middle pier to middle of the arch span. The displacements reach the maximum values at the middle of the first and second arches as 2.13 mm and 1.42 mm, respectively.
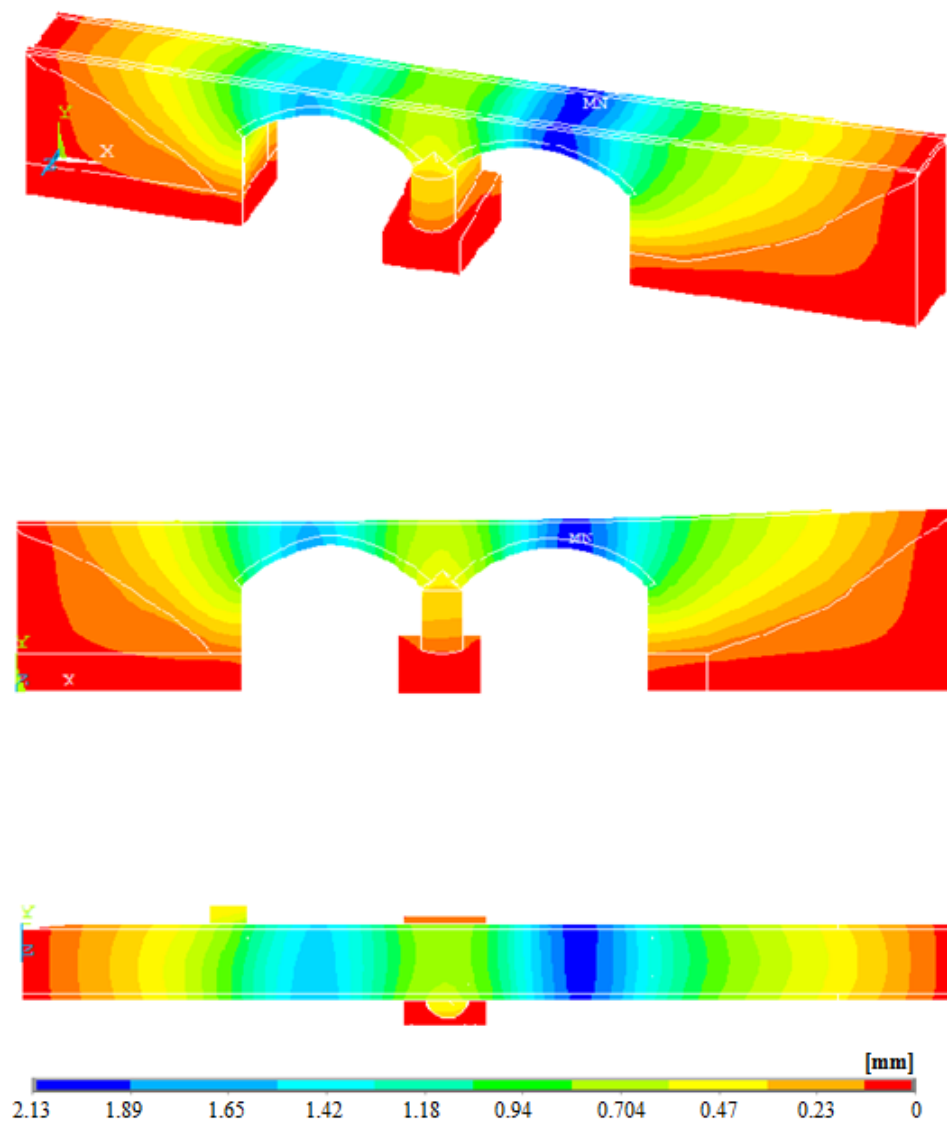
Fig. 5 Maximum displacement contours of the bridge under dead load at current situation (Case 4)

The maximum tensile stress contour diagram of the bridge under dead load at current situation (Case 4) is shown in Fig. 6. It is seen from the Fig. 6 that maximum values of the tensile stresses occurred at contact points between bridge and side supports as 0.72MPa, locally. Also, there are some stress accumulations regions with 0.37MPa maximum stress value at side walls, inner sides of arches and upper side of pier. Excluding these sections, tensile stresses are reached maximum values as 0.18MPa.
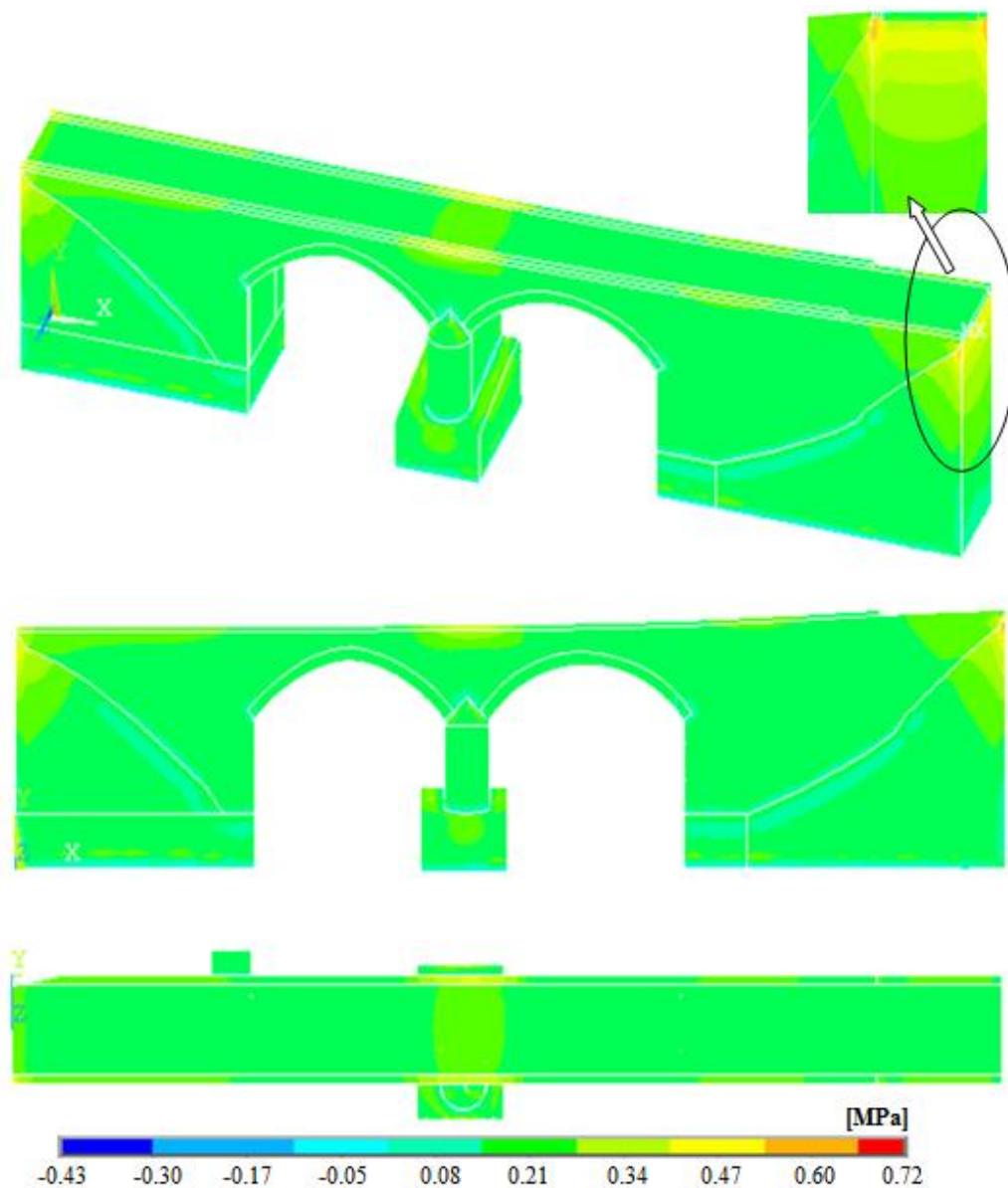
Fig. 6 Maximum tensile stress of the bridge under dead load at current situation (Case 4)

Ahmet C. Altunışık, Burcu Kanbur and Ali F. Genç

The maximum compressive stress contour diagram of the bridge at current situation (Case 4) under dead load is shown in Fig. 7. It is seen from the Fig. 7 that maximum values of the compressive stresses occurred at the damaged side walls and contact surface between the lower parts of arches and pier/side abutments as 2.11MPa, locally. Also, there are some stress accumulations regions with 1.25MPa maximum stress value at the intersection lines between arches and side walls, bottom surface of side slopes and middle pier foundation. Excluding these sections, compressive stresses are reached maximum values as 0.39MPa.
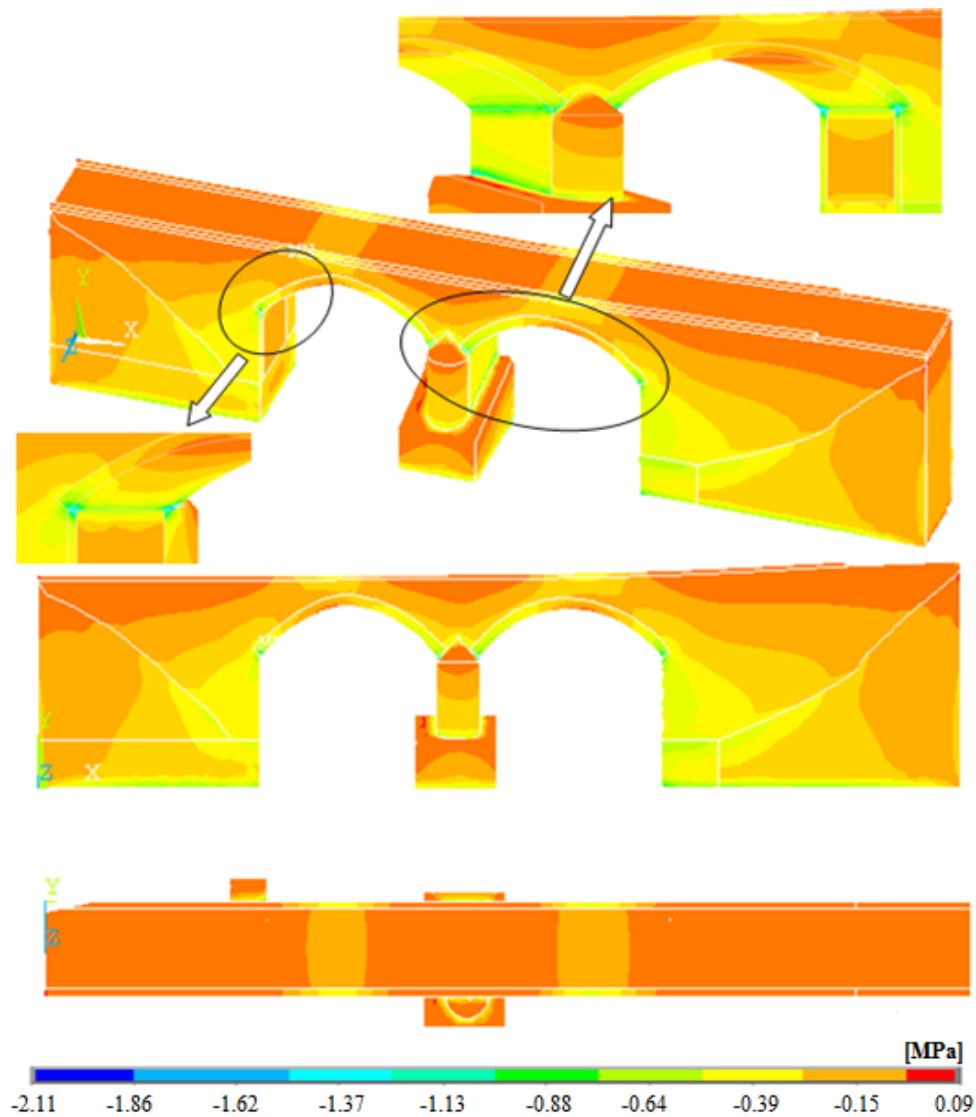

Fig. 7 Maximum compressive stress of the bridge under dead load at current situation (Case 4)

The maximum and minimum elastic strains contour diagrams of the bridge at current situation (Case 4) under dead load are shown in Fig. 8. It is seen from the Fig. 8 that maximum and minimum elastic strains are attained as 0.23E-3 and -0.74E-3, respectively. Also, there are some strain accumulations regions with 0.14E-3 maximum strain value at the damaged side walls, inner sides of arches and upper side of pier. Moreover, there are some strain accumulations regions with 0.16E-3 minimum strain value at the contact surfaces between arches and side walls on pier and pavement.
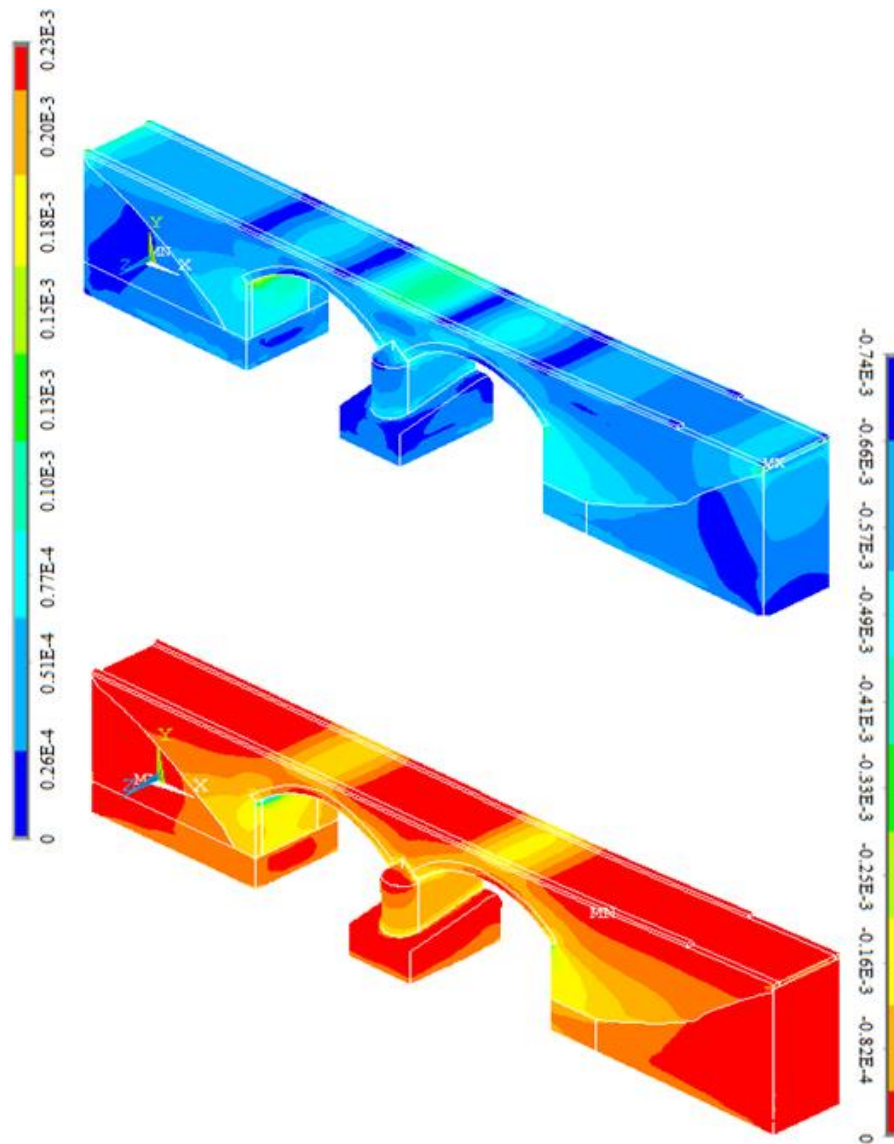

Fig. 8 The elastic strains of the masonry bridge under dead load at current situation

4.2 Structural response under dead and live loads

Structural behavior of the masonry arch bridge is analyzed under dead and live loads in this part of the paper. The live load on the bridge is considered as 1500 kg/m2 for human and vehicle traffic. The maximum vertical displacements contour diagram of the bridge for current situation (Case 4) under dead and live loads is shown in Fig. 9. It can be seen from the Fig. 9 that the displacements have an increasing trend from side abutments and middle pier to middle of the arch span. The displacements reach the maximum values at the middle of the first and second arches as 2.57 mm and 1.99 mm, respectively.
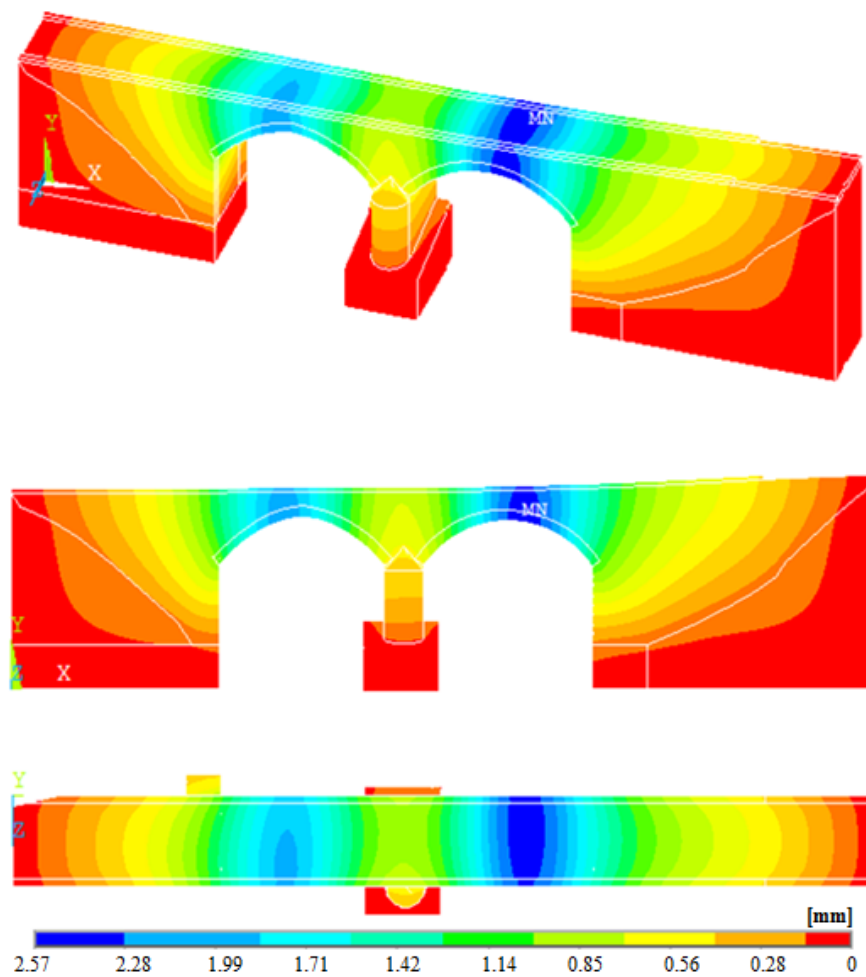

Fig. 9 Maximum displacement contours of the bridge under dead and live loads at current situation (Case 4)

The maximum tensile stress contour diagram of the bridge under dead and live loads at current situation (Case 4) is shown in Fig. 10. It is seen from the Fig. 10 that maximum values of the tensile stresses occurred at contact points between bridge and side supports as 0.83MPa, locally. Also, there are some stress accumulations regions with 0.53MPa maximum stress value at side walls, inner sides of arches and upper side of pier. Excluding these sections, tensile stresses are reached maximum values as 0.22MPa.
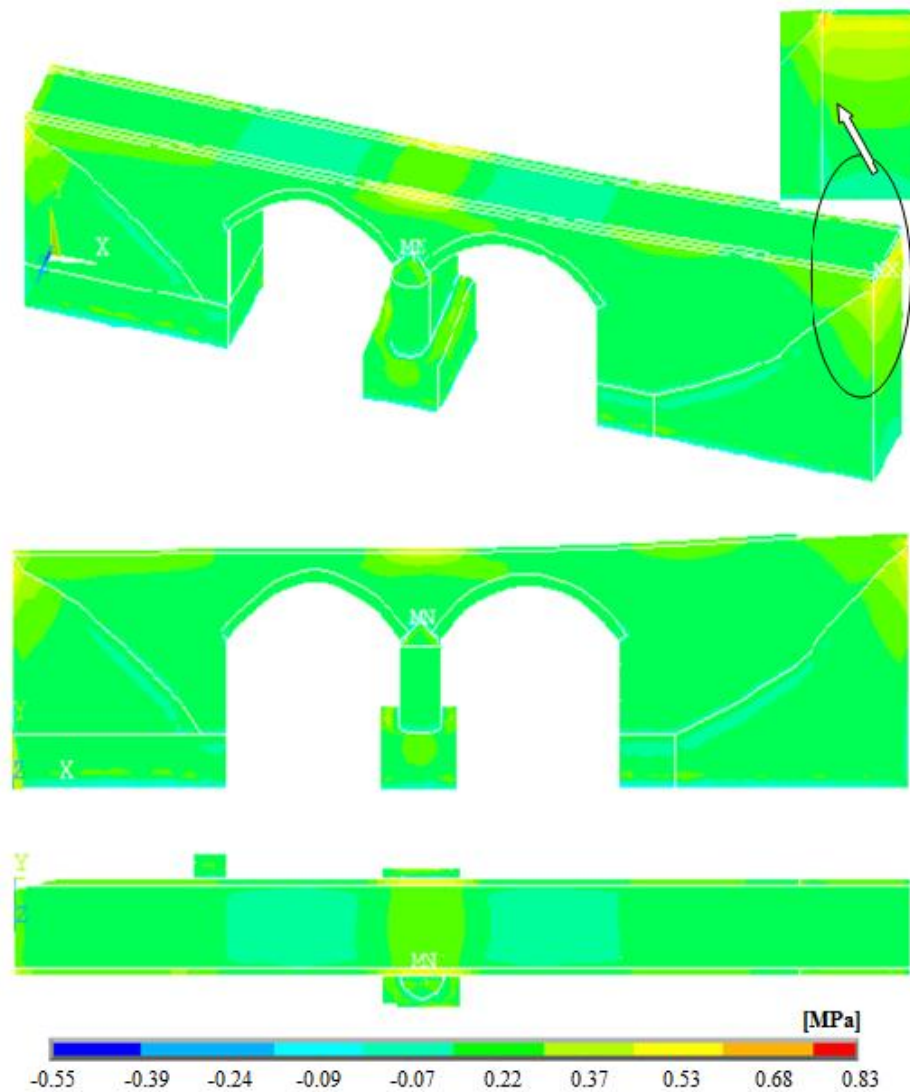

Fig. 10 Maximum tensile stress of the bridge under dead and live loads at current situation (Case 4)

The maximum compressive stress contour diagram of the bridge at current situation (Case 4) under dead and live loads is shown in Fig. 11. It is seen from the Fig. 11 that maximum values of the compressive stresses occurred at the damaged side walls and contact surface between the lower parts of arches and pier/side abutments as 2.60MPa, locally. Also, there are some stress accumulations regions with 1.40MPa maximum stress value at the intersection lines between arches and side walls, bottom surface of side slopes and middle pier foundation. Excluding these sections, compressive stresses are reached maximum values as 0.49MPa.
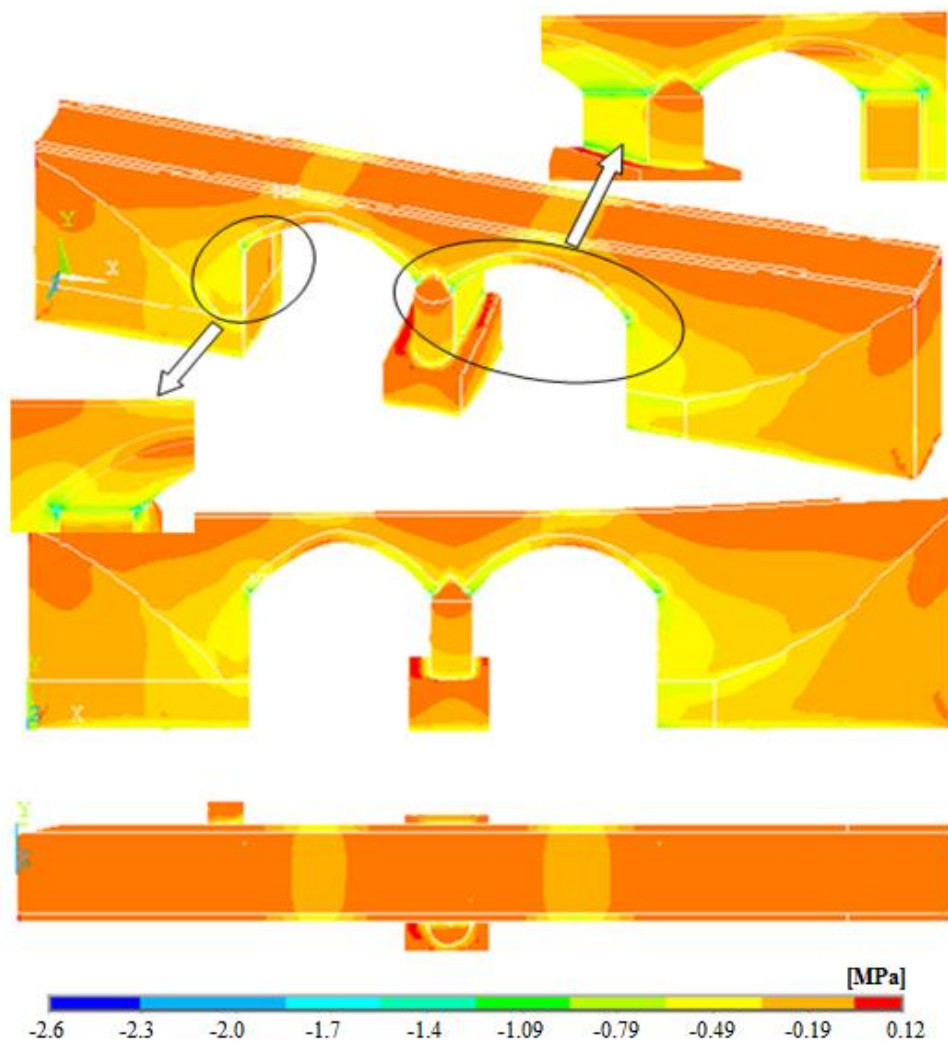

Fig. 11 Maximum compressive stress of the bridge under dead and live loads at current situation (Case 4)

The maximum and minimum elastic strains contour diagrams of the bridge at current situation (Case 4) under dead and live loads are shown in Fig. 12. It is seen from the Fig. 12 that maximum and minimum elastic strains are attained as 0.26E-3 and -0.92E-3, respectively. Also, there are some strain accumulations regions with 0.15E-3 maximum strain value at the damaged side walls, inner sides of arches and upper side of pier. Moreover, there are some strain accumulations regions with -0.61E-3 minimum strain value at the contact surfaces between arches and side walls on pier and pavement.
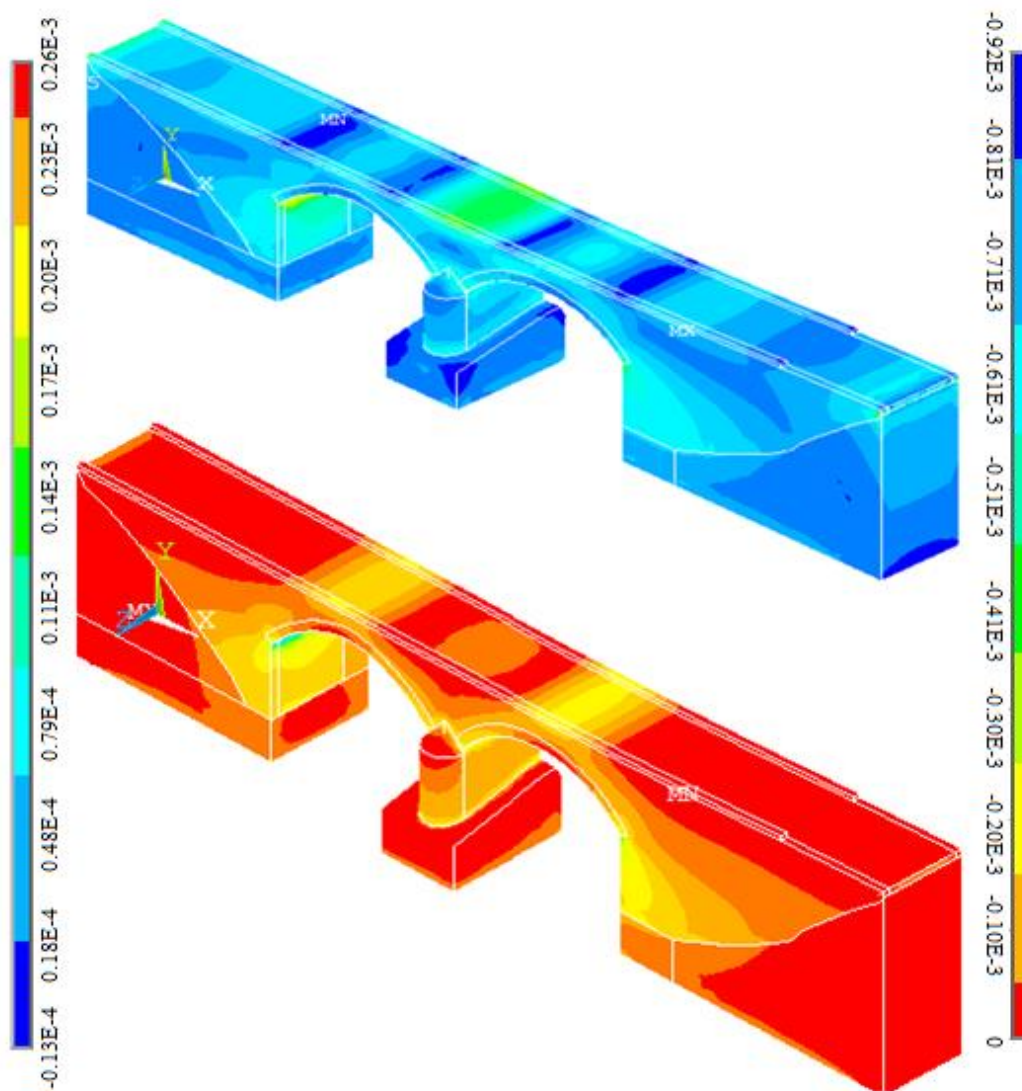
Fig. 12 The elastic strains of the masonry bridge under dead and live loads at current situation

The analyses results considering different arch thickness obtained from the dead and live loads are summarized in Tables 3 and 4. The bold characters are used to imply the peak values which are obtained at the local points and may not be display the real behavior. The normal characters under the bold fonts are used to imply the general distributions of displacements, stresses and strains on the bridge. It is thought that these values can be used to compare the results with limit boundaries.

The changing of maximum displacements, maximum-minimum principal stresses and maximum-minimum elastic strains with different arch thickness under dead and live loads are shown in Figs. 13(a)-13(e).

There is a certain correlation between arch thicknesses and displacements. Maximum displacements decreased nearly about 19.79% and 20.60% for dead and dead-live loads owing to increasing of arch thickness, respectively (Fig. 13(a)). It can be seen that dead load is more effective than live loads on displacements.

From the Fig. 13(b), it is seen that the tensile stress values are nearly equal for all arch thickness under dead loads. The values are decreased from the 0.738MPa to 0.701MPa. Same changing curve are attained for dead-live loads up to Case 7 (0.82 cm-0.99 cm arch thickness). After this point, the values are decreased apparently from 0.817MPa to 0.625MPa and continue same values at the rest. It can be seen that the tensile stresses may lead to cracking or separation.
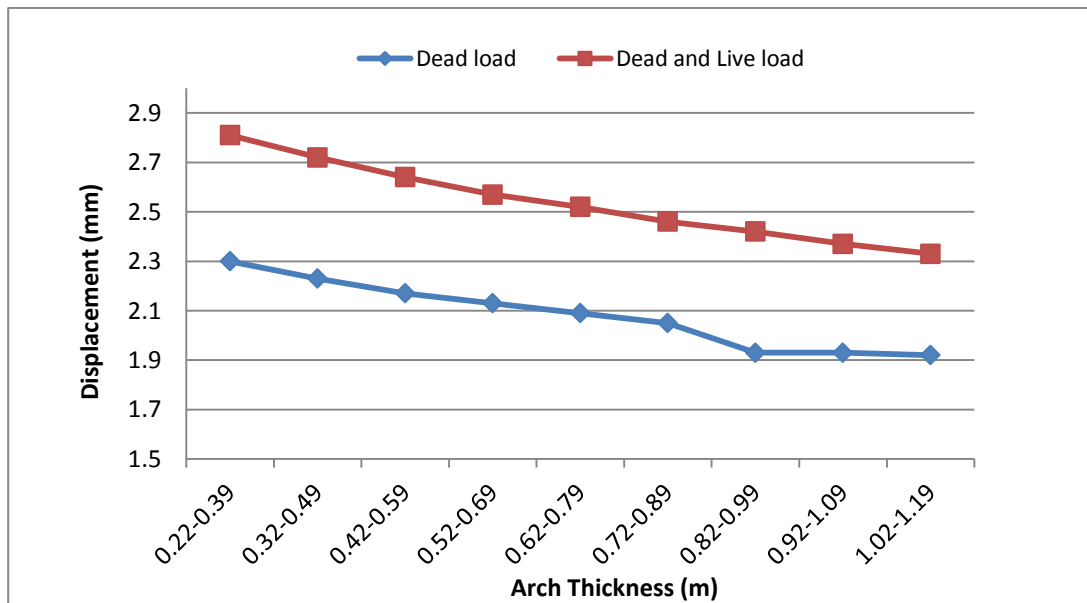
From the Fig. 13(c), it is seen that the compressive stresses are nearly equal and do not change with different arch thickness for dead and dead-live loads. The values increased from 2.03MPa and 2.56MPa to 2.17MPa and 2.72MPa for dead and dead-live loads, respectively.

Table 3 Analyses results for different arch thickness under dead load

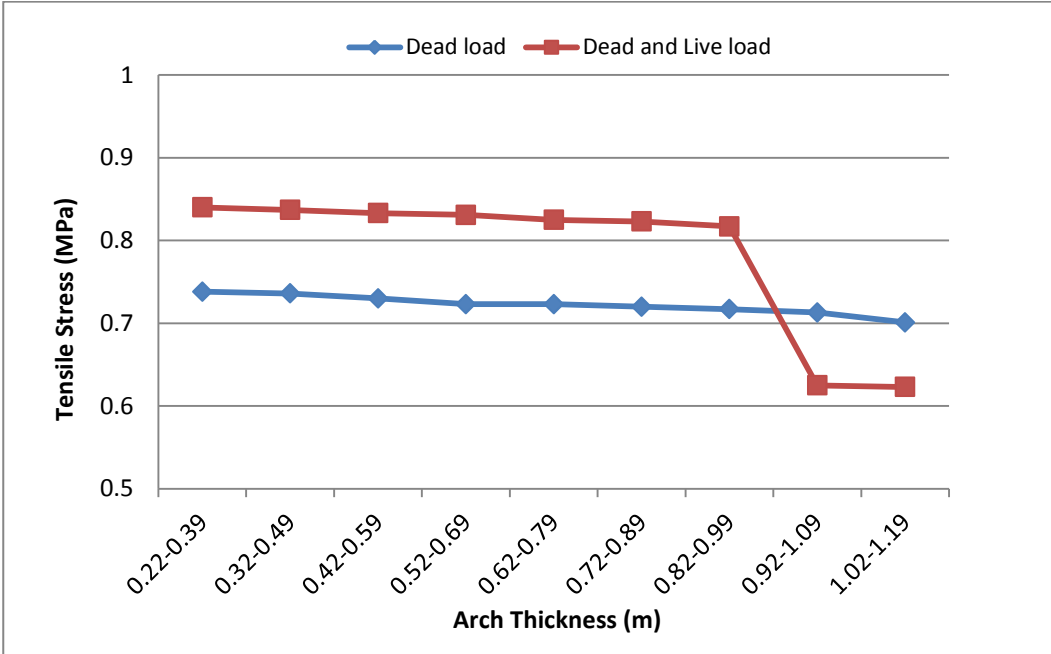| Arch Thicknesses (m) | Analysis Results under Dead Load | | | | |
| | Displacement (mm) | Stresses (MPa) | | Strains (--) | |
		Tension	*Compressive*	*Tension*	*Compressive*
0.22-0.39	**2.30**	**0.738**	**2.03**	**0.242E-3**	**0.68E-3**
		0.088	0.140	0.281E-4	0.75E-4
0.32-0.49	**2.23**	**0.736**	**2.06**	**0.242E-3**	**0.68E-3**
		0.088	0.145	0.280E-4	0.75E-4
0.42-0.59	**2.17**	**0.730**	**2.07**	**0.232E-3**	**0.73E-3**
		0.085	0.125	0.263E-4	0.80E-4
0.52-0.69	**2.13**	**0.723**	**2.11**	**0.232E-3**	**0.74E-3**
		0.083	0.146	0.257E-4	0.823E-4
0.62-0.79	**2.09**	**0.723**	**2.12**	**0.232E-3**	**0.76E-3**
		0.081	0.148	0.256E-4	0.83E-4
0.72-0.89	**2.05**	**0.720**	**2.13**	**0.232E-3**	**0.78E-3**
		0.079	0.150	0.256E-4	0.86E-4
0.82-0.99	**1.93**	**0.717**	**2.15**	**0.232E-3**	**0.79E-3**
		0.075	0.151	0.245E-4	0.87E-4
0.92-1.09	**1.93**	**0.713**	**2.15**	**0.227E-3**	**0.86E-3**
		0.063	0.154	0.244E-4	0.95E-4
1.02-1.19	**1.92**	**0.701**	**2.17**	**0.221E-3**	**0.93E-3**
		0.014	0.157	0.244E-4	0.10E-3

Table 4 Analyses results for different arch thickness under dead and live loads

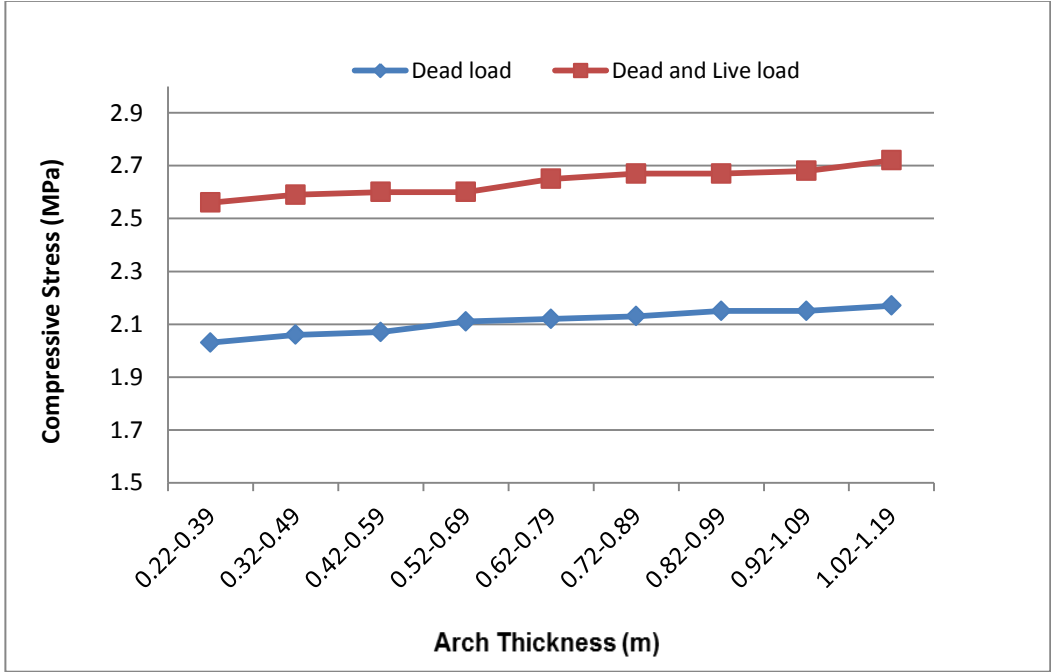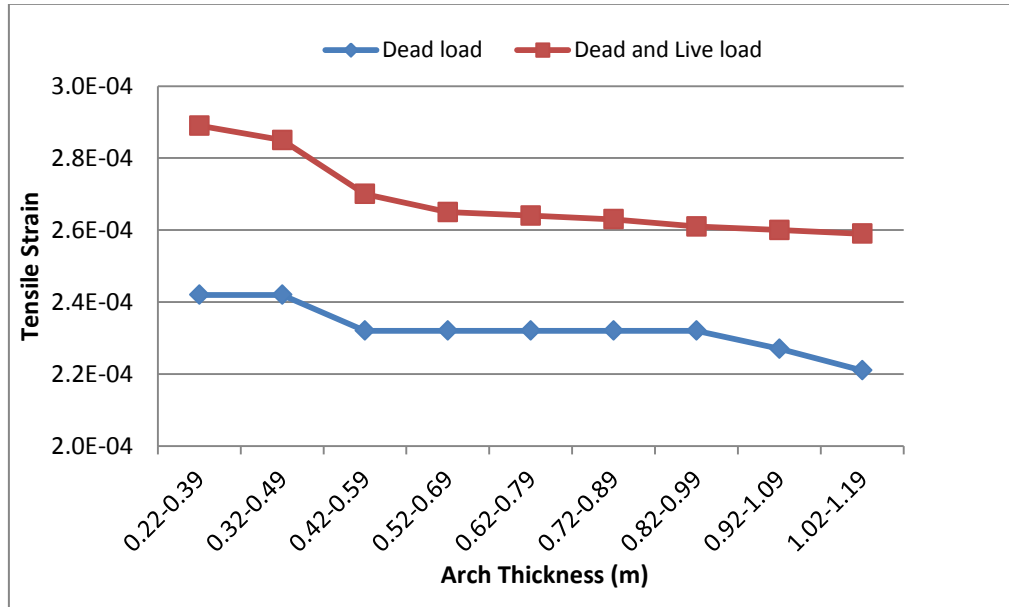| Arch Thicknesses (m)	Analysis Results under Dead and Live Loads				
	Displacement (mm)	Stresses (MPa)		Strains (--)	
		Tension	*Compressive*	*Tension*	*Compressive*
0.22-0.39	**2.81**	**0.840**	**2.56**	**0.289E-3**	**0.841E-3**
		0.065	0.21	0.208E-4	1.011 E-4
0.32-0.49	**2.72**	**0.837**	**2.59**	**0.285E-3**	**0.844E-3**
		0.063	0.215	0.201E-4	1.015E-4
0.42-0.59	**2.64**	**0.833**	**2.60**	**0.270E-3**	**0.909E-3**
		0.062	0.185	0.177E-4	1.089E-4
0.52-0.69	**2.57**	**0.831**	**2.60**	**0.265E-3**	**0.916E-3**
		0.062	0.186	0.175E-4	1.102E-4
0.62-0.79	**2.52**	**0.825**	**2.65**	**0.264E-3**	**0.935E-3**
		0.060	0.194	0.171E-4	1.122E-4
0.72-0.89	**2.46**	**0.823**	**2.67**	**0.263E-3**	**0.962E-3**
		0.059	0.219	0.169E-4	1.158E-4
0.82-0.99	**2.42**	**0.817**	**2.67**	**0.261E-3**	**1.05E-3**
		0.058	0.220	0.167E-4	1.159E-4
0.92-1.09	**2.37**	**0.625**	**2.68**	**0.260E-3**	**1.06E-3**
		0.049	0.224	0.166E-4	1.271E-4
1.02-1.19	**2.33**	**0.623**	**2.72**	**0.259E-3**	**1.12E-3**
		0.032	0.230	0.161E-4	1.350E-4

(a) Maximum displacement

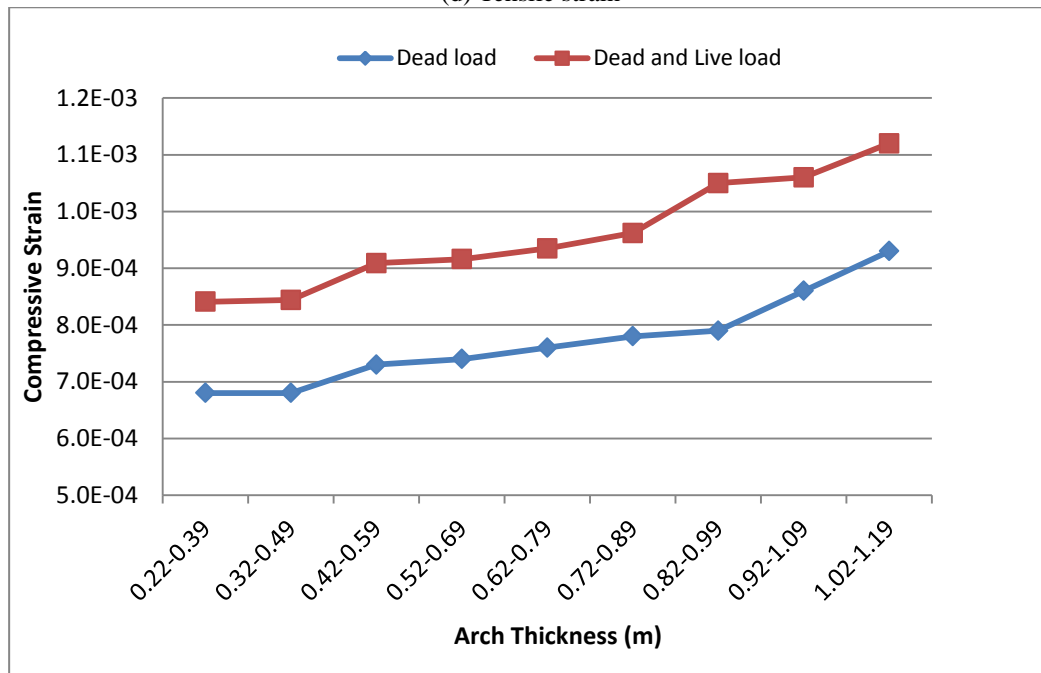Continued-

(b) Tensile stress

(c) Compressive stress

Continued-

(d) Tensile strain

(e) Compression strain

Fig. 13 The changing of maximum displacements, maximum-minimum principal stresses and maximum-minimum elastic strains with different arch thickness under dead and dead-live loads

From the Fig. 13(d), it can be seen that the same tensile strain values are attained for Case 1 and Case 2 considering dead and dead-live loads. After this point, the values are decreased from the 0.242E-3 to 0.232E-3 for dead load and 0.285E-3 to 0.270E-3 for dead-live loads in Case 3. There is no change between Case 3 and Case 7 for dead load, then the curve decrease regularly at a value of 0.221E-3. There is a small decrease between Case 3 to Case 9 for dead-live loads.

From the Fig. 13(e), it is seen that two analysis results have an increasing trend. The values increased from 0.68E-3to 0.93E-3 for dead load and 0.841E-3 to 1.12E-3 for dead-live loads.

5. Conclusions

The aim of this study is to investigate the arch thickness effects on the structural behavior of masonry arch bridges. Finite element model of the Göderni masonry arch bridge is constructed with ANSYS software using relievo drawings. The arch thickness is changed by increasing and decreasing respectively to show the arch thickness effect under dead and dead-live loads. As a result of the study the following observations were made:

- The maximum displacements increased when the arch thicknesses were decreased and this is true for reverse conditions. The maximum displacements occur at the middle of first arch. The maximum displacement increased from 1.92 mm to 2.30 mm and 2.33 mm to 2.81 mm for dead load and dead-live loads analyses respectively.
- The tension stresses increased when the arch thicknesses were decreased for each analysis. Maximum values of the tensile stresses occurred at contact points between bridge and side supports. The tensile stresses increased from 0.701MPa to 0.738MPa and 0.623MPa to 0.840MPa for dead load and dead-live loads analyses respectively. It can be seen that the tensile stresses may lead to cracking or separation.
- The compressive stresses increased dependent on increasing the arch thicknesses. Maximum values of the compressive stresses occurred at the damaged side walls and contact surface between the lower parts of arches and pier/side abutments. The compressive stresses increased from 2.03MPa to 2.17MPa, and 2.56MPa to 2.72MPa for dead load and dead-live loads analyses respectively.
- The tensile strains decreased when the arch thicknesses were increased. The tensile strains decreased from 0.242E-3 to 0.221E-3, and 0.289E-3to 0.259E-3 for dead load and dead-live loads analyses respectively.
- The values of compressive strains increased from 0.68E-3 to 0.93E-3 and 0.841E-3 to 1.12E-3 considering Case 1 and Case 9 for dead and dead-live loads, respectively

Stone and mortar samples are taken from the bridge to determine the mechanical properties of materials used in the bridge and are tested in the laboratory. The compressive strength and weight per unit volume are measured as 30-50MPa and 2000-2400 kg/m^3 for stones, respectively. Also, the compressive strength of the mortar is defined as 4-9MPa.

From the study, it can be seen that the arch thickness influences the structural behavior of the masonry bridge as a vital parameter. This advantage can be used during restoration and repairing practices of the bridges which have exposed high traffic loads in last century while they didn't evaluate for these heavy loads.

References

Altunışık, A.C., Bayraktar, A., Sevim, B. and Birinci, F. (2011), "Vibration-based operational modal analysis of the Mikron historic arch bridge after restoration", *Civil Eng. Environ. Syst.*, **28**(3), 247-259.

ANSYS. (2014), Swanson Analysis System. U.S.A.

Arteaga, I. and Morer, P. (2012), "The effect of geometry on the structural capacity of masonry arch bridges", *Constr. Build.Mater.*, **34**, 97-106.

Bayraktar, A., Altunışık, A.C., Türker, T. and Sevim, B. (2007), "The effect of finite element model updating on earthquake behaviour of historical bridges", *Proceedings of the 6th National Conference on Earthquake Engineering,* Istanbul, Turkey, October.

Bayraktar, A., Birinci, F., Altunışık, A.C., Türker, T. and Sevim, B. (2009), "Finite element model updating of Senyuva historical arch bridge using ambient vibration tests", *Baltic J. Road Bridge Eng.*, **4**(4), 177-185.

Bayraktar, A., Altunışık, A.C., Birinci, F., Sevim, B. and Türker, T. (2010), "Finite element analysis and vibration testing of a two-span masonry arch bridge", *J. Perform. Constr. Fac.*, **24**(1), 46-52.

Brencich, A. and Sabia, D. (2008), "Experimental identification of a multi-span masonry bridge: The Tanaro Bridge", *Constr. Build. Mater.*, **22**, 2087-2099.

Cancelliere, I., Imbimbo, M. and Sacco, E. (2010), "Experimental tests and numerical modeling of reinforced masonry arches", *Eng. Struct.*, **32**, 776-792.

Caporale, A., Feo, L., Hui, D. and Luciano, R. (2014), "Debonding of FRP in multi-span masonry arch structures via limit analysis", *Compos. Struct.*, **108**, 856-865.

Çakir, F. and Uysal, H. (2014), "Experimental modal analysis of brick masonry arches strengthened prepreg composites", *J. Cultural Heritage*, DOI:10.1016/j.culher.2014.06.003.

Frunzio, G., Monaco, M. and Gesualdo, A. (2001), "3D FEM analysis of a Roman Arch Bridge", *Historical Constr.*, 591-598.

Oliveira, D.V., Lourenço, P.B. and Lemos, C. (2010), "Geometric issues and ultimate load capacity of masonry arch bridges from the northwest Iberian Peninsula", *Eng. Struct.*, **32**, 3955-3965.

Pelà, L., Aprile, A. and Benedetti, A. (2013), "Comparison of seismic assessment procedures for masonry arch bridges", *Constr. Build. Mater.*, **38**, 381-394.

Sayın, E., Karaton, M., Yön, B. and Calayır, Y. (2011), "Nonlinear dynamic analysis of historical Uzunok Bridge considering soil-structure interaction", *Proceedings of the 1st Earthquake Engineering and Seismology Conference in Turkey*, Ankara, Turkey.

Sevim, B., Bayraktar, A., Altunışık, A.C., Atamtürktür, S. and Birinci, F. (2011), "Assessment of nonlinear seismic performance of a restored historical arch bridge using ambient vibrations", *Nonlinear Dynam.*, **63**(4), 755-770.

Tao, Y., Stratford, T.J. and Chen, J.F. (2011), "Behaviour of a masonry arch bridge repaired using fibre-reinforced polymer composites", *Eng. Struct.*, **33**, 1594-1606.

Toker, S. and Unay, A.I. (2004), "Mathematical modeling and finite element analysis of masonry arch bridges", *J. Sci. Gazi Univ.*, **17**(2), 129-139.

Ural, A., Oruç, Ş., Doğangün, A. and Tuluk, Ö.İ. (2008), "Turkish historical arch bridges and their deteriorations and failures", *Eng. Fail. Anal.*, **15**, 43-53.

CC